STRUCTURAL CONTROL AND HEALTH MONITORING
Struct. Control Health Monit. 2008; **15**:265–282
Published online 5 February 2008 in Wiley InterScience
(www.interscience.wiley.com) DOI: 10.1002/stc.242

Traffic-induced vibrations on a simple frame: Influence of external action coherence on structural response

S. Pastò*,†, G. Bartoli and L. Facchini

Civil and Environmental Engineering Department, University of Florence, 3, v. S. Marta, 50139 Florence, Italy

SUMMARY

The study of the traffic-induced response of a simple frame structure is presented. In particular, the effect of the spatial correlation, among the traffic-induced ground displacements, is discussed by means of a parametric study to achieve the purpose of outlining those configurations yielding the less-conservative structural response. Ground excitations are estimated by the model of Hunt (*J. Sound Vib.* 1991; **1**:41–51; *J. Sound Vib.* 1991; **1**:53–70) assuming a quarter-car vehicle model moving on an uneven roadway placed on the top of a homogeneous half-space. The structure consists of a rigid slab supported by four columns and subjected by traffic-induced forces suitably condensed in its center of mass. Copyright © 2008 John Wiley & Sons, Ltd.

KEY WORDS: traffic-induced vibrations; coherence; structural response; random dynamics

1. INTRODUCTION

Traffic-induced vibrations on buildings are usually due to heavy vehicles traveling along roads with irregular surfaces. Typical examples are given by the roads of the historic center of cities. The unevenness of a road surface interacts with the wheels of traveling vehicles causing dynamic excitations, due to vehicle mass, suspension system and tyres, which are applied to the roadway and then transmitted to the nearby buildings through soil.

Ground vibrations are of great concern to human beings, above all when they result in dynamic excitations of buildings. The three main areas of concern are building damage, people discomfort and diseases, and malfunction of sensitive equipments. Each area of interest involves

*Correspondence to: S. Pastò, Civil and Environmental Engineering Department, University of Florence, 3, v. S. Marta, 50139 Florence, Italy.
†E-mail: stefanop@dicea.unifi.it

Contract/grant sponsor: MIUR

Received 29 January 2007
Revised 12 November 2007
Accepted 4 December 2007

different levels of peak accelerations, according to the intensity and the frequency contents of traffic-induced vibrations.

To predict traffic-induced ground vibrations acting at the base of structures placed in proximity of a roadway, it is first necessary to define a dynamic vehicle model from which tyre forces may be computed for a given road unevenness profile as a consequence of the dynamic interaction between the same roadway and vehicle. The randomness of road surfaces is suitably described in the frequency domain (see, e.g. [1, 2]), so that the power spectra of the tyre forces, applied to the roadway, are given by filtering the power spectral density of the unevenness by the vehicle admittance function which in turn depends on its dynamic modeling.

Traffic-induced random forces propagate through soil generating spatial ground vibrations which are random processes as well. These ground vibrations may be computed by using the formulas reported in several references starting from the pioneering work of Lamb [3]. At the roadside, these vibrations are non-stationary since the vibrations level rises and falls with the passage of each individual vehicle. In this case, time-dependent power spectra of ground vibrations are needed (see, e.g. [4, 5]). Nevertheless, away from the road, an observer cannot distinguish the passage of a single vehicle; hence, the ground motion may be considered stationary (see e.g. [3, 6]) as well as the forces induced on the above structures. In particular, these forces are generated by the free-field ground displacements acting at the structure base. In more refined models, the assessment of these forces and of their induced structural response also considers the road–soil and the soil–structure interactions, respectively. Whenever these interactions are neglected, the spatial ground displacements are directly imposed on the structure foundations.

Since the spatial components of the ground vibrations occur simultaneously, a key role is played by the mutual correlation among these components when the structural response is being assessed. In the present study, a very simple structure has been modeled with the aim of studying the influence of either large or small coherence among the ground displacements applied to the structure foundation. A parametric study has been performed in the frequency domain assuming stationary loading processes for the sake of simplicity and because this assumption leads to conservative structural responses. No interactions have been considered. The examined structure is composed by a simple rigid slab supported by four columns, and placed 10 m away from a roadway understood as the source of traffic-induced waves propagating all over a free field until the structure base. Such waves, resulting in spatial ground accelerations, have been supposed to be induced by a vehicle traveling along the roadway. The ground accelerations have been modeled by the numerical model of Hunt [6, 7] and then reduced in forces acting at the center of mass of the rigid slab, in order to reduce computational efforts. In particular, the structure response, in terms of slab accelerations, has been computed in the frequency domain considering the spectra of the above forces and defining their cross-spectra by means of a coherence function decaying with the distance among the bases of the columns where the ground accelerations were applied. The higher or lower coherence has been controlled by parameters whose variation has led to a parametric study of the slab accelerations.

2. MODELING OF THE TRAFFIC-INDUCED FORCES AND FRAME RESPONSE

As mentioned above, the traffic-induced ground motion, in terms of displacements or accelerations, acts at the base level of the structure. Contrary to seismic action, traffic-induced

DOI: 10.1002/stc

ground motion does not act uniformly, but the motion components differ from each other in time and space. In the latter case, to assess the structure response it is necessary to evaluate the structure displacement, along its degrees of freedom, induced by each component of the ground motion. It is possible to achieve this aim considering the ground displacements as sinking constraints applied at the base of each column. Since the slab has been supposed to be a rigid plate, the traffic-induced forces may be condensed in its center of mass. Consequently, the spatial displacements of any point of the rigid body may be computed suitably starting from the motion of the slab center of mass by the theory of rigid body, as described later.

The rigid slab may translate and rotate along the spatial coordinates x, y and z defined in Figure 1. The vector of total displacements is given by the sum of its independent movements, $\mathbf{u}_s(t)$, and those induced by the sinking constraints, $\mathbf{u}_c(t)$, that is

$$\mathbf{u}_t(t) = \mathbf{u}_s(t) + \mathbf{u}_c(t) \tag{1}$$

The displacements grouped together in the vector $\mathbf{u}_c(t)$ should be understood as quasi-static, so they may be computed easily by solving the following system of equations:

$$\begin{bmatrix} \mathbf{K}_{ss} & \mathbf{K}_{sg} \\ \mathbf{K}_{sg}^T & \mathbf{K}_{gg} \end{bmatrix} \begin{bmatrix} \mathbf{u}_c(t) \\ \mathbf{u}_g(t) \end{bmatrix} = \begin{bmatrix} 0 \\ \mathbf{f}_g(t) \end{bmatrix} \tag{2}$$

where $\mathbf{K}_{ss}$ and $\mathbf{K}_{gg}$ are the stiffness matrices related to

$$\mathbf{u}_s(t) = [u_{5,x}(t), u_{5,y}(t), u_{5,z}(t), \varphi_{5,x}(t), \varphi_{5,y}(t), \varphi_{5,z}(t)]^T \tag{3}$$

and

$$\mathbf{u}_g(t) = [u_{1,x}(t), \ldots, u_{1,z}(t), \varphi_{1,x}(t), \ldots, \varphi_{1,z}(t), \ldots, u_{4,x}(t), \ldots, u_{4,z}(t), \ldots, \varphi_{4,x}(t), \varphi_{4,z}(t)]^T \tag{4}$$

respectively, whereas $\mathbf{K}_{sg}$ is the matrix composed by the elastic forces induced along $\mathbf{u}_s(t)$ by $\mathbf{u}_g(t)$ which themselves are supposed to be generated by the unknown forces $\mathbf{f}_g(t)$.

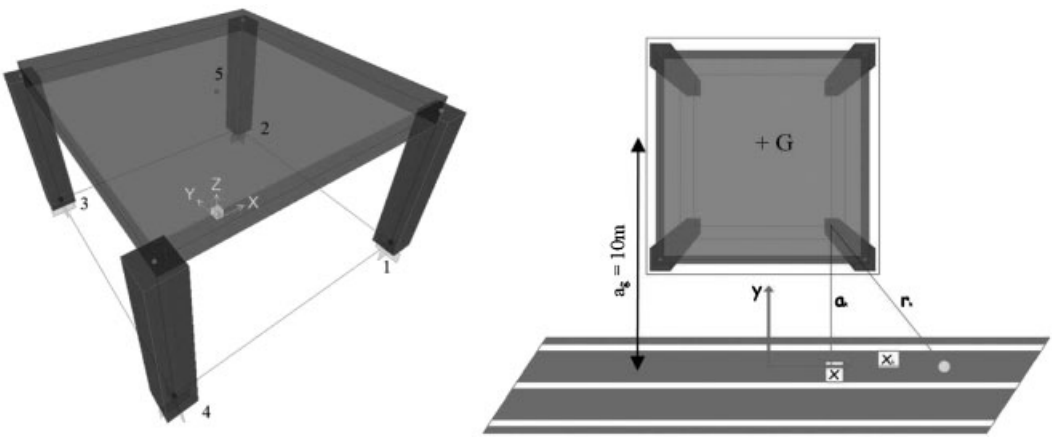

Figure 1. Illustration of the scheme of the structure (left) supposed to be placed near a roadway (right).

DOI: 10.1002/stc

The system of equations in Equation (2) may be solved easily to obtain

$$\mathbf{u}_c(t) = -\mathbf{K}_{ss}^{-1}\mathbf{K}_{sg}\mathbf{u}_g(t) = \mathbf{K}_{ss}^{-1}\mathbf{f}_s(t) \tag{5}$$

where $\mathbf{f}_s(t) = -\mathbf{K}_{sg}\mathbf{u}_g(t)$ are the quasi-static forces induced by the ground motion. In this way, neglecting the soil–structure interaction, the dynamic response of the slab may be computed by solving the well-known problem below:

$$\mathbf{M}_{ss}\ddot{\mathbf{u}}_s + \mathbf{C}_{ss}\dot{\mathbf{u}}_s + \mathbf{K}_{ss}\mathbf{u}_s(t) = \mathbf{f}_s(t) \tag{6}$$

In the frequency domain, the problem in Equation (6) enables to assess the power spectral density matrix of the response $\mathbf{S}_{u_s u_s}(\omega)$:

$$\mathbf{S}_{u_s u_s}(\omega) = \mathbf{A}\mathbf{H}(\omega)\mathbf{S}_{f_s f_s}(\omega)\mathbf{H}^*(\omega)\mathbf{A}^T \tag{7}$$

where $\mathbf{A}$ is the structure eigenmodes matrix (see Figure 2),

$$\mathbf{A} = [\mathbf{a}_1, \ldots, \mathbf{a}_6] \tag{8}$$

whereas $\mathbf{H}(\omega)$ is the structural admittance as a function of the angular frequency ω, given the modal mass, m_i, the ith natural angular frequency of the structure, ω_i, and the modal damping ration v_i:

$$\mathbf{H}(\omega) = \begin{bmatrix} H_1(\omega) & \ldots & 0 \\ \vdots & \ddots & \vdots \\ 0 & \ldots & H_6(\omega) \end{bmatrix}, \quad H_i(\omega) = \frac{1}{m_i\omega_i^2\left[1 - \left(\frac{\omega}{\omega_i}\right)^2 + 2jv_i\left(\frac{\omega}{\omega_i}\right)\right]} \tag{9}$$

$\mathbf{H}^*(\omega)$ is the complex conjugate of $\mathbf{H}(\omega)$. Finally, the power spectral density matrix of the traffic-induced forces is given taking the Fourier transform of the cross-correlation function matrix of $\mathbf{f}_s(t) = -\mathbf{K}_{sg}\mathbf{u}_g(t)$, that is

$$\mathbf{S}_{f_s f_s}(\omega) = \mathbf{K}_{sg}(\omega)\mathbf{S}_{u_g u_g}(\omega)\mathbf{K}_{sg}^T \tag{10}$$

where $\mathbf{S}_{u_g u_g}(\omega)$ is given by the model of Hunt [6, 7] and in the present case it writes as follows:

$$\mathbf{S}_{u_g u_g}(\omega) = \begin{bmatrix} \mathbf{S}_{x_1x_1}(\omega) & 0 & 0 & \ldots & 0 & 0 & 0 \\ \vdots & \ddots & \vdots & \ldots & \vdots & \vdots & \vdots \\ 0 & 0 & \mathbf{S}_{x_4x_4}(\omega) & 0 & 0 & 0 & 0 \\ \vdots & \vdots & \vdots & \ddots & \vdots & \vdots & \vdots \\ 0 & 0 & 0 & 0 & \mathbf{S}_{z_1z_1}(\omega) & 0 & 0 \\ \vdots & \vdots & \vdots & \ldots & \vdots & \ddots & \vdots \\ 0 & 0 & 0 & \ldots & 0 & 0 & \mathbf{S}_{z_4z_4}(\omega) \end{bmatrix} \tag{11}$$

DOI: 10.1002/stc

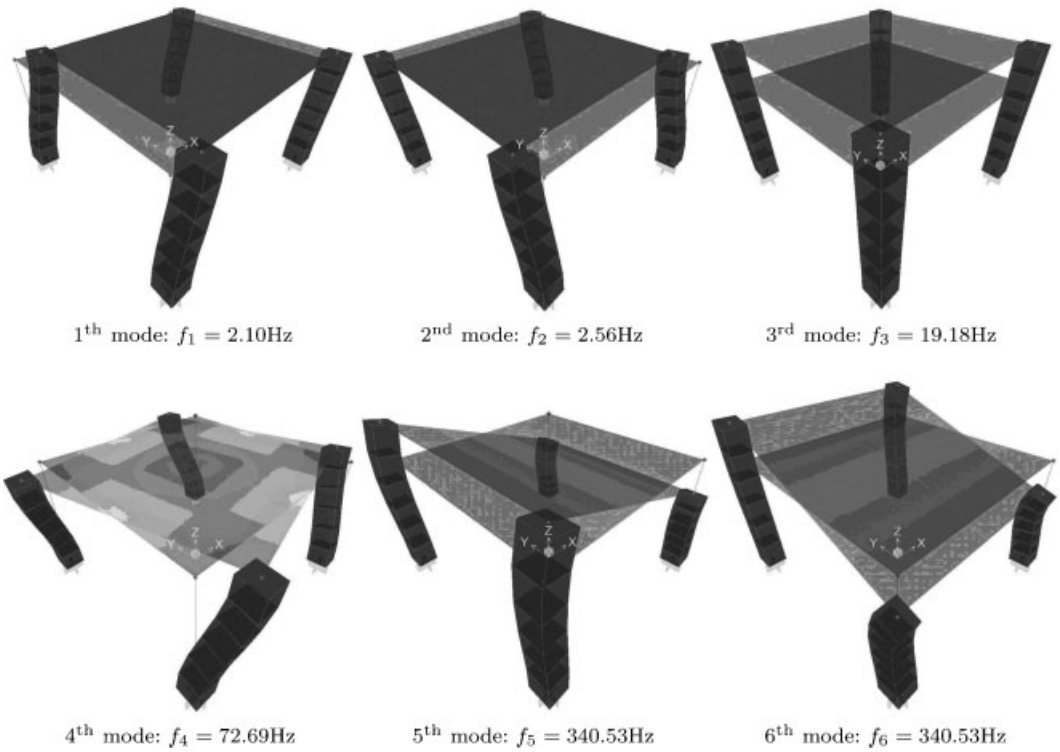

Figure 2. Structure natural modes of vibration and respective frequencies.

For instance, the power spectral density of the traffic-induced ground displacement along x of the point 1 of the structure (see Figure 1) is given by

$$S_{x_1x_1}(\omega) = |H_{xf}(x_1, \omega)|^2 S_{ff}(\omega) \tag{12}$$

where $S_{ff}(\omega)$ is the power spectrum of the force applied on the roadway surface because of its random unevenness and $|H_{xf}(x, \omega)|^2$ is the ground admittance along the directions x. The latter quantities, however, will be discussed in details later.

3. POWER SPECTRAL DENSITY OF THE VEHICLE-INDUCED FORCES

The vehicle is modeled as a single-degree-of-freedom system as shown in Figure 3. The force induced on the roadway may be formulated in the frequency domain starting from the definition of the vehicle frequency response function. As a first approach, assume that $m = M_1$, $M_2 = 0$, $c_1 = c_2 = 0$, $k = k_1 + k_2$ and $x = x_1$, in the vehicle model shown in Figure 3. The system response to a harmonic profile of the road unevenness, $x_p(t) = Y(\omega)e^{j\omega t}$, will be $x = X(\omega)e^{j\omega t}$; hence, the frequency response function may be derived easily as

$$H_{xy}(\omega) = X(\omega)/Y(\omega) = 1/[1 - (\omega/\omega_n)^2] \tag{13}$$

DOI: 10.1002/stc

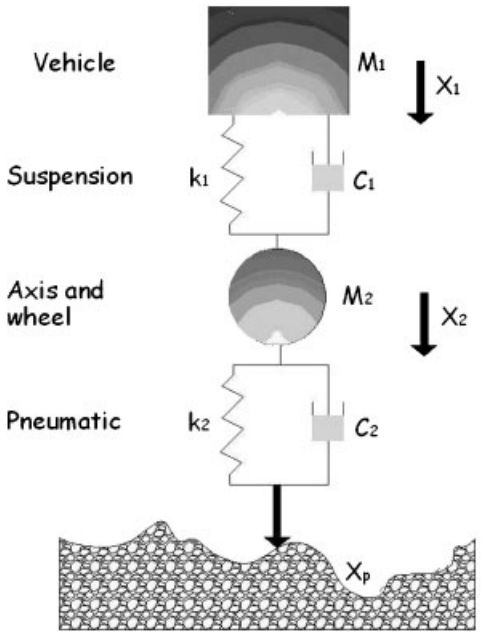

Figure 3. Illustration of the vehicle dynamic system: M_1 is the vehicle mass, k_1 and c_1 are, respectively, the suspension stiffness and damping, M_2 is the unsuspended mass, k_2 and c_2 are, respectively, the pneumatic stiffness and damping, x_p is the ground height variation.

where ω_n is the vehicle natural angular frequency. As a consequence of $x_p(t)$, the vehicle exerts on the roadway an inertial force, $f(t) = -m\ddot{x}(t)$, whose frequency response function can be expressed as

$$H_{fy}(\omega) = F(\omega)/Y(\omega) = -m\omega^2/[1 - (\omega/\omega_n)^2] \tag{14}$$

The power spectrum of the applied forces due to a random profile is then given by the following formula:

$$S_{ff}(\omega) = |H_{fy}(\omega)|^2 S_{YY}(\omega) \tag{15}$$

The expression in Equation (15) means that the spectrum of the road profile, $S_{YY}(\omega)$, is filtered by the vehicle admittance function, $|H_{fy}(\omega)|^2$.

In the case of the two-degrees-of-freedom system in Figure 3, it is possible to derive the vehicle admittance function in a similar way. In particular, the system motion is governed by the following system of differential equations:

$$M_1\ddot{x}_1(t) + c_1(\dot{x}_1(t) - \dot{x}_2(t)) + k_1(x_1(t) - x_2(t)) = 0$$

$$M_2\ddot{x}_2(t) + c_2\dot{x}(t) + k_2x_2(t) - c_1(\dot{x}_1(t) - \dot{x}_2(t)) - k_1(x_1(t) - x_2(t)) = c_2\dot{x}_p(t) + k_2x_p(t) \tag{16}$$

Because of the roadway unevenness, the force that the system exerts on the roadway is

$$f(t) = [M_1\ddot{x}_1(t) + M_2\ddot{x}_2(t)] = M\ddot{Z}(t) \tag{17}$$

DOI: 10.1002/stc

where $M = M_1 + M_2$ and $\ddot{Z} = [M_1\ddot{x}_1(t) + M_2\ddot{x}_2(t)]/M$ is the weighted-mean acceleration. By considering a harmonic excitation $x_p(t) = Y e^{i\omega t}$ and response, $X_1 e^{i\omega t}$ and $X_2 e^{i\omega t}$, the equations in Equation (16) may be rewritten in the following form:

$$\begin{bmatrix} A_{11} & A_{12} \\ A_{21} & A_{22} \end{bmatrix} \begin{bmatrix} X_1 \\ X_2 \end{bmatrix} = \begin{bmatrix} 0 \\ B_2 \end{bmatrix} Y \tag{18}$$

where

$$\mu = \frac{M_2}{M_1}, \quad v_1 = \frac{c_1}{2\sqrt{k_1 M_1}}, \quad v_2 = \frac{c_2}{2\sqrt{k_2 M_2}}$$

$$\omega_1 = \sqrt{\frac{k_1}{M_1}}, \quad \omega_2 = \sqrt{\frac{k_2}{M_2}}, \quad \alpha = \frac{\omega_2}{\omega_1}, \quad \beta = \frac{v_2}{v_1}, \quad \Omega = \frac{\omega}{\omega_1}$$

$$A_{11} = -\Omega^2 + 2iv_1\Omega + 1, \quad A_{12} = -(2iv_1\Omega + 1), \quad A_{12} = A_{21}$$

$$A_{22} = -\mu\Omega^2 + 2i(\mu\alpha\beta + 1)v_1\Omega + (\mu\alpha^2 + 1), \quad B_2 = 2i\mu\alpha\beta v_1\Omega + \mu\alpha^2 \tag{19}$$

By inverting the matrix in Equation (19), we can express:

$$\begin{bmatrix} X_1 \\ X_2 \end{bmatrix} = \frac{1}{\Delta} \begin{bmatrix} A_{22} & -A_{12} \\ -A_{21} & A_{11} \end{bmatrix} \begin{bmatrix} 0 \\ B_2 \end{bmatrix} Y \tag{20}$$

where $\Delta = A_{11}A_{22} - A_{12}A_{21}$. By fixing the parameter $\mu = M_2/M_1$, it is possible to see from Equations (19) and (20) that the vehicle frequency response is independent of the total vehicle mass, M, but it is dependent only on M_1; hence, the force exerted on the roadway (see Equation (17)) may be rewritten as

$$f(t) = M_1\ddot{Z}(t) \tag{21}$$

whereas the weighted acceleration is given by the following expression:

$$\ddot{Z} = (M_1\ddot{X}_1 + M_2\ddot{X}_2)/M_1 = (\ddot{X}_1 + \mu\ddot{X}_2) = \omega^2(X_1 + \mu X_2) = \omega^2 \frac{B_2}{\Delta}(A_{12} - \mu A_{11})Y \tag{22}$$

From Equation (22) it is possible to distinguish the vehicle response function for the two-degrees-of-freedom system:

$$H_{\ddot{Z}Y}(\omega) = \omega^2 \frac{B_2}{\Delta}(A_{12} - \mu A_{11}) \tag{23}$$

Consequently, the power spectrum of the vehicle-induced force due to a random road profile is finally expressed as

$$S_{ff}(\omega) = \frac{M_1^2}{V}|H_{\ddot{Z}Y}(\omega)|^2 S_{YY}(\gamma) \tag{24}$$

where $\gamma = \omega/V$ is the spatial wave number of road surface roughness and V is the vehicle velocity.

DOI: 10.1002/stc

4. POWER SPECTRAL DENSITY OF THE ROAD PROFILE

The road surface profile is assumed, as suggested by the International Standard Organization [2], to be a Gaussian random process defined by the power spectrum:

$$S_{YY}(\gamma) = \begin{cases} S_{YY_0}(\gamma/\gamma_0)^{-n_1}, & \gamma \leqslant \gamma_0 \\ S_{YY_0}(\gamma/\gamma_0)^{-n_2}, & \gamma > \gamma_0 \end{cases} \tag{25}$$

where γ represents the wave number of the road profile (γ being related to wavelength $\lambda = 2\pi/\gamma$). The choice of S_{YY_0}, γ_0, n_1 and n_2 depends on the surface quality (see [2]).

For a vehicle moving at a speed V along the uneven road, the power spectrum of the displacement of the tyre contact point can be expressed as

$$S_{YY}(\omega) = \frac{1}{V} S_{YY}(\gamma = \omega/V) \tag{26}$$

as reported in [8].

5. THE HALF-SPACE FREQUENCY RESPONSE FUNCTION

The homogeneous isotropic damped half-space model employed in the current paper is based on the works of Lamb [3]. It neglects the vehicle–roadway interaction.

Disturbances in an homogenous isotropic half-space propagate through it as compressive and shear waves, and as Rayleigh waves along the surface. These three wave types travel at speeds c_1, c_2 and c_r, respectively. In detail, one obtains

$$c_1 = \sqrt{(G/\rho)2(1-\nu)/(1-2\nu)}, \quad c_2 = \sqrt{G/\rho} \tag{27}$$

where G, ν and ρ are, respectively, the elastic shear modulus, the Poisson ratio and the density of the half-space. The Rayleigh wave speed, c_r, cannot be expressed explicitly in terms of G, ν and ρ, but a method to compute it may be found in [3].

Shear and compressive waves both decay inversely as the square of distance from a point of excitation, whereas Rayleigh waves decay as the square root of distance. Accordingly, the surface response is progressively dominated by Rayleigh waves.

The frequency–response functions of a damped system may be obtained by extending those obtained by Lamb [3] for an elastic half-space. In particular, the half-space frequency–response functions found by Lamb, along the spatial coordinate x, y and z, are expressed as follows:

$$H_{xf}(x,\omega) \approx \frac{x}{r}\frac{\omega H}{2\rho c_r^3} H_1^{(2)}\left(\frac{\omega r}{c_r}\right)$$

$$H_{yf}(a,\omega) \approx -\frac{a}{r}\frac{\omega H}{2\rho c_r^3} H_1^{(2)}\left(\frac{\omega r}{c_r}\right) \tag{28}$$

$$H_{zf}(z,\omega) \approx \frac{\omega K}{2\rho c_r^3} H_0^{(2)}\left(\frac{\omega r}{c_r}\right)$$

DOI: 10.1002/stc

where $r = \sqrt{a^2 + x^2}$ (see Figure 1), ρ is the half-space density, H and K are material constants depending on the Lamé constants of the half-space.

Within the elastic–viscoelastic analogy (see, e.g. [9]), the shear modulus, Poisson ratio and bulk modulus are written as complex quantities $G^*(\omega) = G + \mathrm{i}\omega G'(\omega)$, $v^*(\omega) = v + \mathrm{i}\omega v'(\omega)$, $k^* \times (\omega) = k + \mathrm{i}\omega k'(\omega)$, where the real parts of the complex moduli are not functions of frequency. The damping properties of a homogeneous isotropic solid are uniquely defined by specifying any two of $G'(\omega)$, $v'(\omega)$ and $k'(\omega)$. Usually, it is possible to assume that $G^*(\omega) = G(1 + \mathrm{i}\omega D(\omega))$ as well as $k^*(\omega) = k(1 + \mathrm{i}\omega D(\omega))$, where $D = G'(\omega)/G = k'(\omega)/k$.

In the case in which the bulk damping is zero, the complex shear and bulk moduli may be expressed as

$$G^* = G(1 + \mathrm{i}\omega D), \quad k^* = k \tag{29}$$

Accordingly, the Poisson ratio v^* may be derived to obtain

$$v^* \approx v - \mathrm{i}\omega D \tfrac{1}{3}(1 + v)(1 - 2v) \tag{30}$$

in the case of light damping ($D \ll 1$).

The elastic–viscoelastic analogy may be used to find the frequency–response functions for a damped half-space from those derived for an elastic half-space and defined by Equation (28). In particular, G^*, v^*, c_r, K and H are changed by small amounts ∂G^*, ∂v^*, ∂c_r, ∂K and ∂H, respectively. Here, for the sake of brevity, the final results, derived by Hunt [6], are reported:

$$H_{xf}(x, \omega) \approx \frac{x}{r}\frac{\omega H}{2\rho c_r^3}\exp\left[-\frac{Dr\omega^2}{2c_r}H_1^{(2)}\left(\frac{\omega r}{c_r}\right)\right]$$

$$H_{yf}(a, \omega) \approx -\frac{a}{r}\frac{\omega H}{2\rho c_r^3}\exp\left[-\frac{Dr\omega^2}{2c_r}H_1^{(2)}\left(\frac{\omega r}{c_r}\right)\right] \tag{31}$$

$$H_{zf}(z, \omega) \approx \frac{\omega K}{2\rho c_r^3}\exp\left[-\frac{Dr\omega^2}{2c_r}H_0^{(2)}\left(\frac{\omega r}{c_r}\right)\right]$$

Finally, the power spectra of the traffic-induced ground displacements are given by the following formulas:

$$S_{xx}(\omega) = |H_{xf}(x, \omega)|^2 S_{ff}(\omega)$$

$$S_{yy}(\omega) = |H_{yf}(a, \omega)|^2 S_{ff}(\omega) \tag{32}$$

$$S_{zz}(\omega) = |H_{zf}(z, \omega)|^2 S_{ff}(\omega)$$

where $S_{ff}(\omega)$ is given by Equation (24). Hence, looking at Equation (32), it is possible to summarize the origin of traffic-induced ground displacements in this way: the force induced by the roadway profile is filtered by the vehicle-force admittance function to give a dynamic force acting on the roadway at the tyre–road point of contact (see Equation (24)). This force induces vibrations that propagate through soil. These vibrations are the result of the further filtering process given by the same soil (see Equation (32)).

DOI: 10.1002/stc

6. COHERENCE EFFECT OF THE TRAFFIC-INDUCED FORCES ON THE FRAME RESPONSE

A vehicle (characterized by $\omega_1 = 18.8\,\text{rad/s}$, $\mu = 0.15$, $\alpha = 5.5$, $\beta = 7.5$, $v = 0.04$) has been supposed to transit by a velocity $V = 30\,\text{m/s}$ covering a distance $-100\,\text{m} \leqslant x \leqslant 100\,\text{m}$ along a roadway, placed at a distance equal to $a = 10\,\text{m}$ from the middle of the frame (see Figure 1). The roadway itself has been supposed to be in good condition, so that $S_{YY} = 3.18 \times 10^{-7}\,\text{m}^2/\text{rad/m}$ ($\gamma_0 = 1\,\text{rad/s}$, $n_1 = 2$, $n_2 = 1$). Moreover, the vibrations induced by the passing vehicle propagate until the frame base in a ground characterized by the following quantities: $\rho = 2000\,\text{kg/m}^3$, $H = 0.072$, $K = 0.099$, $c_r = 214\,\text{m/s}$ and $D = 0.00035$.

In Figure 4 the power spectra of the ground displacements induced by the vehicle transit are shown. In particular, the spectra show a peak at the vehicle angular frequency, ω_1, around which the most part of the energy is concentrated. Moreover, the spectra broaden at higher frequencies where the frequency contents of the soil admittance are larger. As it is possible to presume intuitively at first, the more the distance of the vehicle on the roadway, the lower the energy content of the spectra of the ground displacements, as shown in the spectrograms of Figure 4.

6.1. Frame response

The frame response has been evaluated in terms of the standard deviation of the slab accelerations $[\widetilde{\ddot{u}}_x, \widetilde{\ddot{u}}_y, \widetilde{\ddot{u}}_z, \widetilde{\ddot{\varphi}}_x, \widetilde{\ddot{\varphi}}_y, \widetilde{\ddot{\varphi}}_z]$, which are composed using the SRSS method (see, e.g. Chopra [10]). In particular, the total accelerations, along x, y and z, of a certain point on the slab border is derived from the standard relations of a rigid body:

$$\widetilde{a}_x = \sqrt{\widetilde{\ddot{u}}_x^2 + \left(\widetilde{\ddot{\varphi}}_z \frac{L_s}{2}\right)^2}, \quad \widetilde{a}_y = \sqrt{\widetilde{\ddot{u}}_y^2 + \left(\widetilde{\ddot{\varphi}}_z \frac{L_s}{2}\right)^2}, \quad \widetilde{a}_z = \sqrt{\widetilde{\ddot{u}}_z^2 + \left(\widetilde{\ddot{\varphi}}_x \frac{L_s}{2}\right)^2 + \left(\widetilde{\ddot{\varphi}}_y \frac{L_s}{2}\right)^2} \tag{33}$$

where $L_s = 10\,\text{m}$ is the side of the square slab, and

$$\widetilde{\ddot{u}}_i = \sqrt{\int_{-\infty}^{+\infty} \omega^4 S_{u_i u_i}(\omega)\,\mathrm{d}\omega}, \quad i = x, y, z, \quad \widetilde{\ddot{\varphi}}_i = \sqrt{\int_{-\infty}^{+\infty} \omega^4 S_{\varphi_i \varphi_i}(\omega)\,\mathrm{d}\omega}, \quad i = x, y, z \tag{34}$$

where $S_{u_i u_i}(\omega)$ and $S_{\varphi_i \varphi_i}(\omega)$ are the diagonal components of the power spectral density matrix in Equation (7).

6.2. Studied cases

The frame response has been evaluated in different configurations differing from each other for the coherence imposed to ground displacements. The slab accelerations have been computed varying the power spectral density matrix of the ground displacements, $\mathbf{S}_{\mathrm{u_g u_g}}(\omega)$. In particular,

DOI: 10.1002/stc

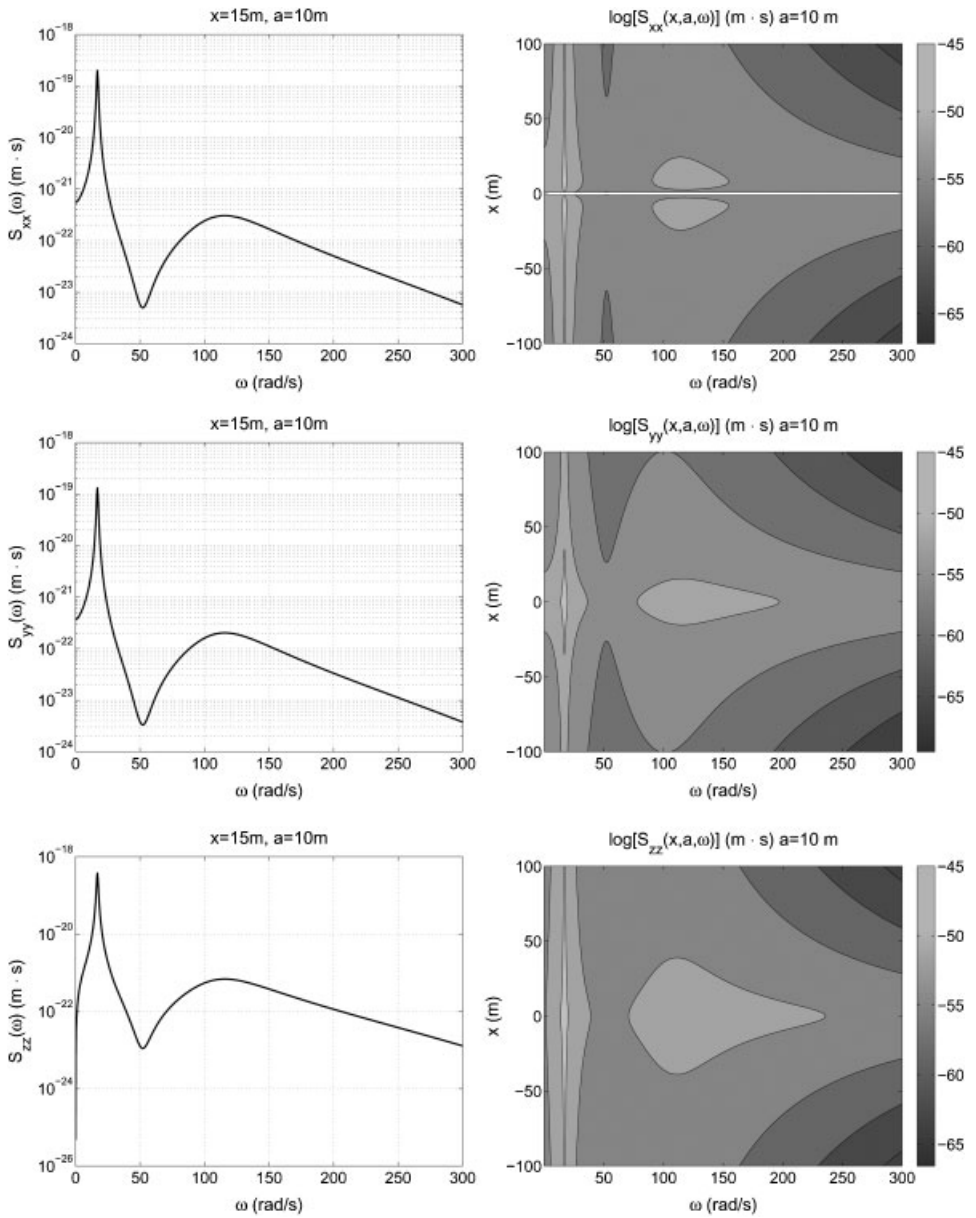

Figure 4. Power spectra of ground displacements: (left) $S_{xx}(\omega)$, $S_{yy}(\omega)$, $S_{zz}(\omega)$ induced by a vehicle passing along a roadway ($x = 10$ m and $a = 10$ m); (right) spectrograms of $S_{xx}(\omega)$, $S_{yy}(\omega)$, $S_{zz}(\omega)$ induced by a vehicle traveling along a roadway ($-100\,\text{m} \leqslant x \leqslant 100\,\text{m}$, $a = 10$ m).

DOI: 10.1002/stc

the ground displacements have been supposed to be:

(A1) All uncorrelated among each other

$$\mathbf{S}_{\mathrm{u_g u_g}} = \begin{bmatrix} \mathbf{S}_{\mathrm{u_{g,x} u_{g,x}}} & \mathbf{0} & \mathbf{0} \\ \mathbf{0} & \mathbf{S}_{\mathrm{u_{g,y} u_{g,y}}} & \mathbf{0} \\ \mathbf{0} & \mathbf{0} & \mathbf{S}_{\mathrm{u_{g,z} u_{g,z}}} \end{bmatrix} \quad \mathbf{S}_{\mathrm{u_{g,}i u_{g,}i}} = \begin{bmatrix} \mathbf{S}_{i_1 i_1} & \dots & \mathbf{0} \\ \vdots & \ddots & \vdots \\ \mathbf{0} & \dots & \mathbf{S}_{i_4 i_4} \end{bmatrix}, \quad i = x, y, z \tag{35}$$

(A2) Correlated along their respective directions, but uncorrelated among orthogonal directions

$$\mathbf{S}_{\mathrm{u_g u_g}} = \begin{bmatrix} \mathbf{S}_{\mathrm{u_{g,x} u_{g,x}}} & \mathbf{0} & \mathbf{0} \\ \mathbf{0} & \mathbf{S}_{\mathrm{u_{g,y} u_{g,y}}} & \mathbf{0} \\ \mathbf{0} & \mathbf{0} & \mathbf{S}_{\mathrm{u_{g,z} u_{g,z}}} \end{bmatrix} \quad \mathbf{S}_{\mathrm{u_{g,}i u_{g,}i}} = \begin{bmatrix} \mathbf{S}_{i_1 i_1} & \dots & \mathbf{S}_{i_1 i_4} \\ \vdots & \ddots & \vdots \\ \mathbf{S}_{i_4 i_1} & \dots & \mathbf{S}_{i_4 i_4} \end{bmatrix}, \quad i = x, y, z \tag{36}$$

(A3) Equal along their respective directions (like a seismic action), but uncorrelated among orthogonal directions

$$\mathbf{S}_{\mathrm{u_g u_g}} = \begin{bmatrix} \mathbf{S}_{\mathrm{u_{g,x} u_{g,x}}} & \mathbf{0} & \mathbf{0} \\ \mathbf{0} & \mathbf{S}_{\mathrm{u_{g,y} u_{g,y}}} & \mathbf{0} \\ \mathbf{0} & \mathbf{0} & \mathbf{S}_{\mathrm{u_{g,z} u_{g,z}}} \end{bmatrix} \quad \mathbf{S}_{\mathrm{u_{g,}i u_{g,}i}} = \begin{bmatrix} \mathbf{S}_{i_5 i_5} & \dots & \mathbf{S}_{i_5 i_5} \\ \vdots & \ddots & \vdots \\ \mathbf{S}_{i_5 i_5} & \dots & \mathbf{S}_{i_5 i_5} \end{bmatrix}, \quad i = x, y, z \tag{37}$$

(A4) Correlated among each other along all directions

$$\mathbf{S}_{\mathrm{u_g u_g}} = \begin{bmatrix} \mathbf{S}_{\mathrm{u_{g,x} u_{g,x}}} & \mathbf{S}_{\mathrm{u_{g,x} u_{g,y}}} & \mathbf{S}_{\mathrm{u_{g,x} u_{g,z}}} \\ \mathbf{S}_{\mathrm{u_{g,y} u_{g,x}}} & \mathbf{S}_{\mathrm{u_{g,y} u_{g,y}}} & \mathbf{S}_{\mathrm{u_{g,y} u_{g,z}}} \\ \mathbf{S}_{\mathrm{u_{g,z} u_{g,x}}} & \mathbf{S}_{\mathrm{u_{g,z} u_{g,y}}} & \mathbf{S}_{\mathrm{u_{g,z} u_{g,z}}} \end{bmatrix} \quad \mathbf{S}_{\mathrm{u_{g,}i u_{g,}j}} = \begin{bmatrix} \mathbf{S}_{i_1 i_1} & \dots & \mathbf{S}_{i_1 j_4} \\ \vdots & \ddots & \vdots \\ \mathbf{S}_{j_4 i_1} & \dots & \mathbf{S}_{i_4 i_4} \end{bmatrix}, \quad i, j = x, y, z \tag{38}$$

(A5) Correlated among each other along all directions, but $\mathbf{S}_{\mathrm{u_{g,x} u_{g,y}}}(\omega) = \mathbf{0}$

$$\mathbf{S}_{\mathrm{u_g u_g}} = \begin{bmatrix} \mathbf{S}_{\mathrm{u_{g,x} u_{g,x}}} & \mathbf{0} & \mathbf{S}_{\mathrm{u_{g,x} u_{g,z}}} \\ \mathbf{0} & \mathbf{S}_{\mathrm{u_{g,y} u_{g,y}}} & \mathbf{S}_{\mathrm{u_{g,y} u_{g,z}}} \\ \mathbf{S}_{\mathrm{u_{g,z} u_{g,x}}} & \mathbf{S}_{\mathrm{u_{g,z} u_{g,y}}} & \mathbf{S}_{\mathrm{u_{g,z} u_{g,z}}} \end{bmatrix} \quad \mathbf{S}_{\mathrm{u_{g,}i u_{g,}j}} = \begin{bmatrix} \mathbf{S}_{i_1 i_1} & \dots & \mathbf{S}_{i_1 j_4} \\ \vdots & \ddots & \vdots \\ \mathbf{S}_{j_4 i_1} & \dots & \mathbf{S}_{i_4 i_4} \end{bmatrix}, \quad i, j = x, y, z \tag{39}$$

(A6) Correlated among each other along all directions, but $\mathbf{S}_{\mathrm{u_{g,x} u_{g,z}}}(\omega) = \mathbf{S}_{\mathrm{u_{g,y} u_{g,z}}}(\omega) = \mathbf{0}$

$$\mathbf{S}_{\mathrm{u_g u_g}} = \begin{bmatrix} \mathbf{S}_{\mathrm{u_{g,x} u_{g,x}}} & \mathbf{S}_{\mathrm{u_{g,x} u_{g,y}}} & \mathbf{0} \\ \mathbf{S}_{\mathrm{u_{g,y} u_{g,x}}} & \mathbf{S}_{\mathrm{u_{g,y} u_{g,y}}} & \mathbf{0} \\ \mathbf{0} & \mathbf{0} & \mathbf{S}_{\mathrm{u_{g,z} u_{g,z}}} \end{bmatrix} \quad \mathbf{S}_{\mathrm{u_{g,}i u_{g,}j}} = \begin{bmatrix} \mathbf{S}_{i_1 i_1} & \dots & \mathbf{S}_{i_1 j_4} \\ \vdots & \ddots & \vdots \\ \mathbf{S}_{j_4 i_1} & \dots & \mathbf{S}_{i_4 i_4} \end{bmatrix}, \quad i, j = x, y, z \tag{40}$$

DOI: 10.1002/stc

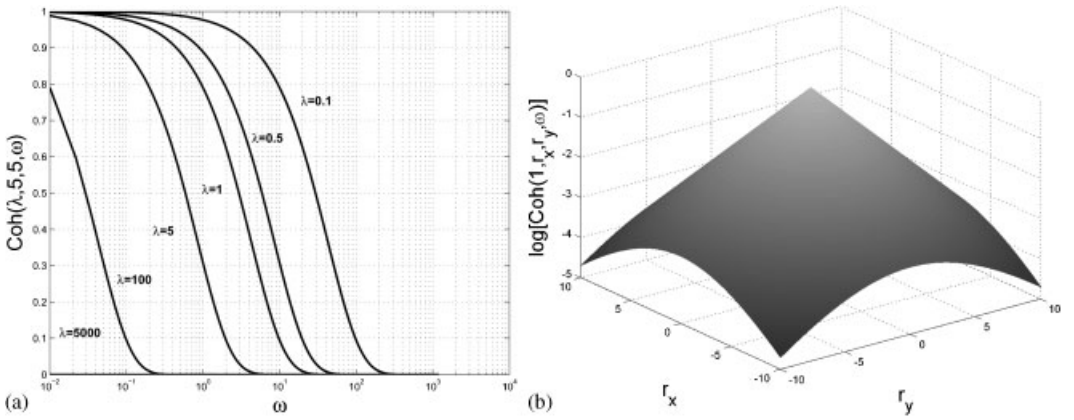

Figure 5. Illustration of the coherence function: (a) coherence decay varying λ and (b) coherence decay varying r_x and r_y.

As it is possible to see, with the exception of the configuration A1, all the other configurations are characterized by different cross-spectral densities among ground displacements. Such cross-spectra are defined introducing the coherence function:

$$\mathbf{S}_{i_h j_k}(\omega) = \sqrt{\mathbf{S}_{i_h i_h}(\omega)\mathbf{S}_{j_k j_k}(\omega)}\,\mathrm{Coh}(\lambda, r_x, r_y, \omega), \quad i,j = x,y,z, \;\; h,k = 1,\ldots,4 \tag{41}$$

The coherence function itself depends on the distance between two column bases, r_x and r_y, on the angular frequency, ω, and on a decay parameter, λ:

$$\mathrm{Coh}(\lambda, r_x, r_y, \omega) = \exp\left(-\frac{\omega\lambda}{V}\sqrt{r_x^2 + r_y^2}\right) \tag{42}$$

The coherence function is shown in Figure 5. If r_x and r_y are fixed, the coherence effect depends only by λ, given ω. In particular, the lower the λ, the higher the coherence between two ground displacements. Two limit cases may be discussed to understand the coherence sensitiveness varying λ. Whenever $\lambda \to 0$ then $\mathrm{Coh}(\omega, \lambda) \to 1$, it means that the frequency contents of $\mathbf{S}_{i_h i_h}(\omega)$ and $\mathbf{S}_{j_k j_k}(\omega)$ (see Equation (41)) act simultaneously by their own magnitudes. On the other hand, whenever $\lambda \to +\infty$ then $\mathrm{Coh}(\omega, \lambda) \to 0$ and $\mathbf{S}_{i_h j_k}(\omega) \to 0$ as well (see Equation (41)), it means that the frequency contents of $\mathbf{S}_{i_h i_h}(\omega)$ and $\mathbf{S}_{j_k j_k}(\omega)$ act separately by their own magnitudes.

7. DISCUSSION OF RESULTS

The slab accelerations, $\widetilde{a}_x$, $\widetilde{a}_y$, $\widetilde{a}_z$ within the configuration A1 (see Equation (35)) are shown in Figure 6. As it is possible to see, the three accelerations are comparable with each other. This testifies that unlike the seismic action, the traffic-induced vertical response, $\widetilde{a}_z$, is important as well. Moreover, it is dutiful to focus on the fact that the ground displacements are completely uncorrelated with each other, so they trigger higher values of $\widetilde{\ddot{\varphi}}_x$, $\widetilde{\ddot{\varphi}}_y$ and $\widetilde{\ddot{\varphi}}_z$, which themselves

DOI: 10.1002/stc

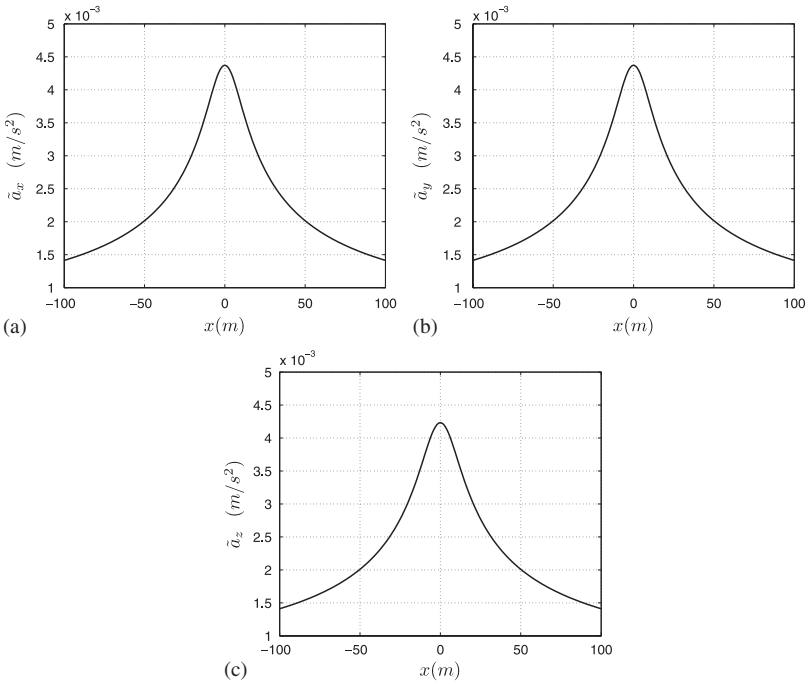

Figure 6. Illustration of the slab accelerations $\widetilde{a}_x$, $\widetilde{a}_y$ and $\widetilde{a}_z$ within configuration A1.

amplify the total displacements (see Equation (33)). Within the configuration A2 (see Equation (35)), it is possible to deduce that the lower the correlation (higher values of λ) among the ground displacements, acting along the same direction, the higher the slab accelerations (see Figure 7). This circumstance may be attributed to the greater capability of the slab to rotate around x, y and z, whenever λ is large. In fact, decreasing the decay parameter of the coherence function, the ground displacements tend to be fully correlated, hence $\widetilde{\ddot{\varphi}}_x$, $\widetilde{\ddot{\varphi}}_y$ and $\widetilde{\ddot{\varphi}}_z$, along the whole slab, decrease since they are more in-phase with each other, despite they are different. On the other hand, increasing the decay parameter the slab accelerations increase and tend asymptotically to the values obtained in the configuration A1, where the complete lack of coherence has been considered (see Figure 6). The slab accelerations, however, are comparable to each other (see Figure 7); hence, the vertical acceleration still assumes a key role in the assessment of the frame response.

A seismic-like action has been modeled within configuration A3 where all the ground displacements at the pillar base have been supposed to be equal to the traffic-induced ground displacement at the projection of the slab center of mass on the foundation base ($a_G = 10$ m, see Figure 1). In this configuration the slab rotations around x, y and z are completely inhibited; hence, its accelerations decrease. In this configuration, the vertical acceleration is predominant (see Figure 8). Further analysis has been carried out even imposing a certain coherence among the traffic-induced ground displacements acting along the orthogonal directions (configurations A4, A5 and A6, see Equations (38)–(40)). In these configurations, the coherence function of the ground displacements acting along the same directions is characterized by the decay parameter

DOI: 10.1002/stc

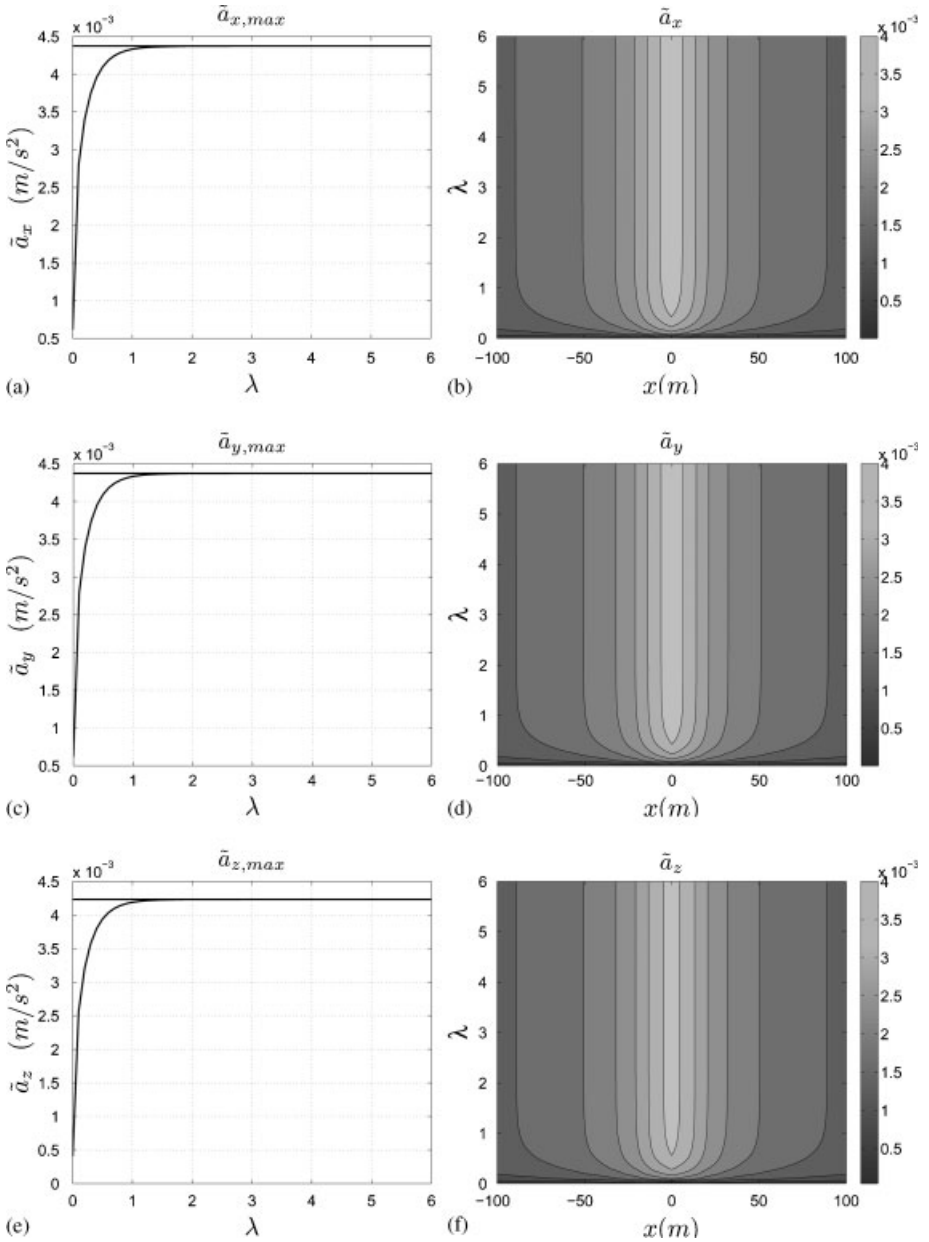

Figure 7. Illustration of the slab accelerations within configuration A2. Left: $\widetilde{a}_x$, $\widetilde{a}_y$ and $\widetilde{a}_z$ varying the coherence decay parameter λ. Right: spectrograms of $\widetilde{a}_x$, $\widetilde{a}_y$ and $\widetilde{a}_z$ varying λ and the position of the vehicle along the roadway (along x).

DOI: 10.1002/stc

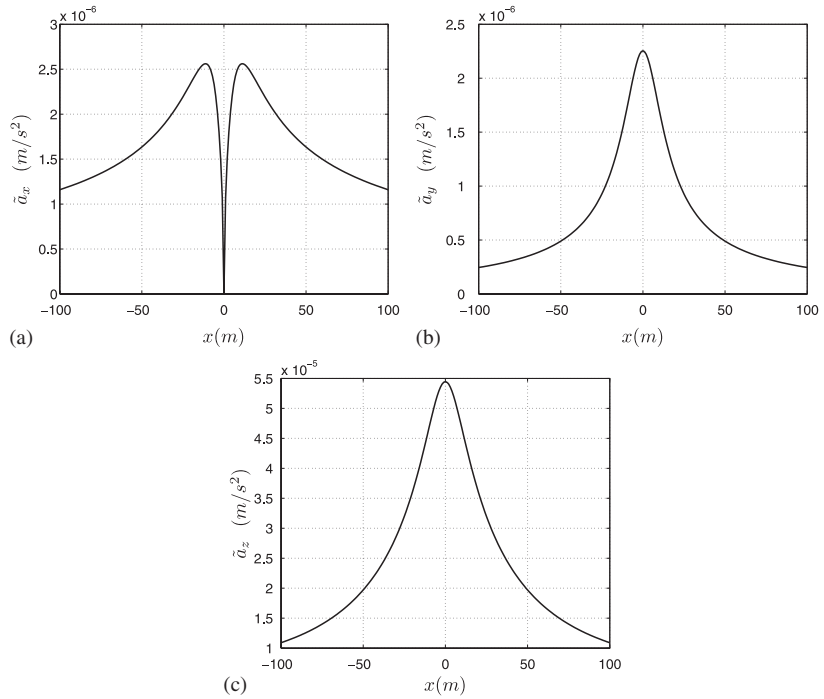

Figure 8. Illustration of the slab accelerations $\tilde{a}_x$, $\tilde{a}_y$ and $\tilde{a}_z$ within configuration A3.

λ, whereas η is the decay parameter of the coherence function among orthogonal ground displacements. These correlation functions, however, are always given by Equation (42), respectively. The results of the three configurations are practically identical (see Figure 9) and yield the conclusion that the slab response is independent of the correlation between the orthogonal traffic-induced ground displacements acting at the frame base.

8. CONCLUSIONS

It is possible to conclude that the correlation between the traffic-induced forces acting on the same direction provides less-conservative results. In the case of a real structure extending along wider surfaces, the coherence tends to vanish as long as the distance between two ground displacements increases (see Figure 5). Nevertheless, it is likewise evident that the knowledge of the real correlation might decrease the structural response which itself sometimes could be too conservative neglecting the coherence completely. The main effect of the traffic-induced forces is triggering slab rotations, which contributes to increase the slab accelerations in comparison with seismic-like actions. On the other hand, the correlation of the forces acting along orthogonal directions does not affect the structure response, at least in the case of simple frames like the frame studied here.

DOI: 10.1002/stc

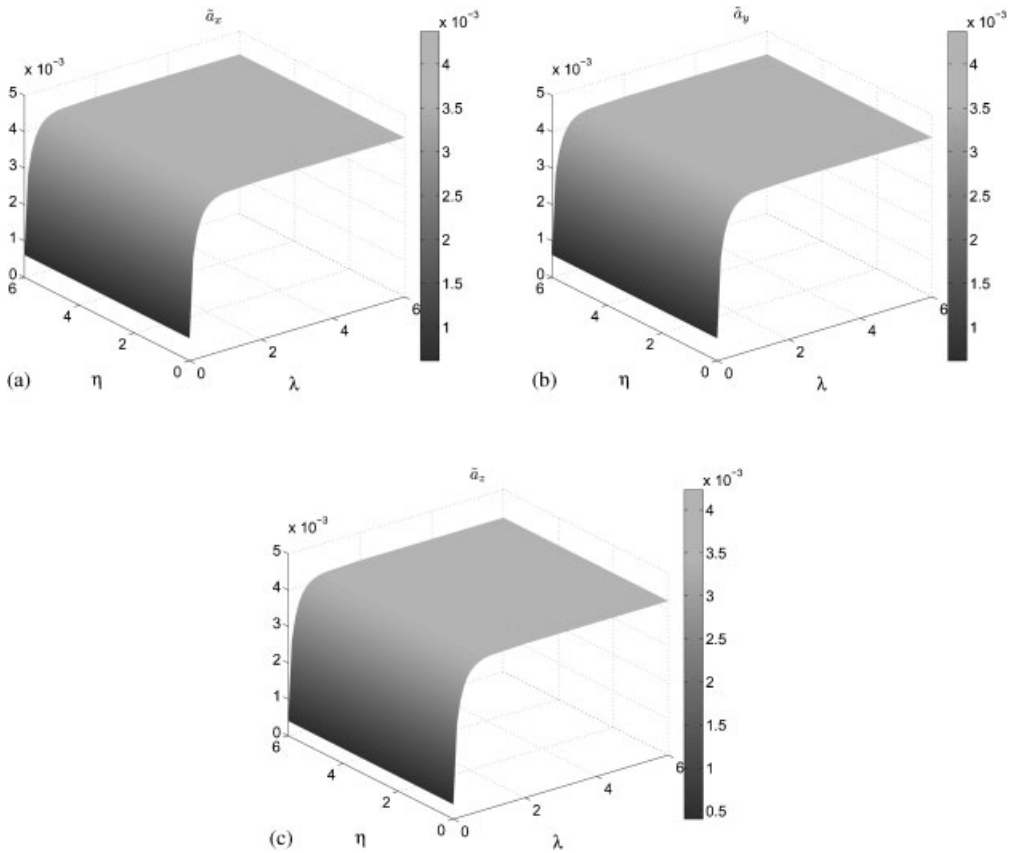

Figure 9. Illustration of the slab accelerations $\tilde{a}_x$, $\tilde{a}_y$ and $\tilde{a}_z$ within configurations A3, A4 and A6. λ is the decay parameter of the coherence function among parallel directions; η is the decay parameter of the coherence function among orthogonal directions.

ACKNOWLEDGEMENTS

The work has been supported by a grant from MIUR, Italian Ministry for Education, University and Research, in the framework of the PRIN 2004 research programme 'VINCES: Vibrations in Civil Engineering Structures: source of damage and discomfort, diagnostic and safety assessment tool'.

REFERENCES

1. Dodds CJ, Robson JD. The description of road surface roughness. *Journal of Sound and Vibration* 1973; **1**:175–183.
2. International Standard Organization (ISO). *Standard 8608*: *Mechanical Vibration*, *Road Surface Profiles*, *Reporting of Measured Data*. International Standard Organization (ISO), 1995.
3. Lamb H. On the propagation of tremors over the surface of an elastic solid. *Philosophical Transactions of the Royal Society of London*, *Series A* 1904; **203**:1–42.
4. Lombaert G, Degrande G, Cloteau D. Deterministic and stochastic modelling of free field traffic induced vibrations. *International Symposium on the Environmental Impact of Road Pavement Unevenness*, Porto, Portugal, vol. 1, March 1999; 163–176.

DOI: 10.1002/stc

5. Lombaert G, Degrande G, Cloteau D. Numerical modelling of free field traffic-induced vibrations. *Journal of Soil Dynamics and Earthquake Engineering* 2000; **19**:473–488.
6. Hunt HEM. Stochastic modelling of traffic induced ground vibration. *Journal of Sound and Vibration* 1991; **1**:53–70.
7. Hunt HEM. Modelling of road vehicles for calculation of traffic induced ground vibrations. *Journal of Sound and Vibration* 1991; **1**:41–51.
8. Newland DE. *An Introduction to Random Vibration and Spectral Analysis* (2nd edn). Longman: New York, 1984.
9. Bland DR. *The Theory of Linear Viscoelasticity*. Academic Press: New York, 1973.
10. Chopra AK. *Dynamic of Structures*: *Theory and Applications to Earthquake Engineering*. Prentice-Hall: Englewood Cliffs, NJ, 2000.

DOI: 10.1002/stc